

# Two Circular Wilson Loops and Marginal Deformations

Changhyun Ahn

*Department of Physics, Kyungpook National University, Taegu 702-701, Korea*

ahn@knu.ac.kr

## Abstract

We study type IIB supergravity backgrounds which are dual to marginal deformations of  $\mathcal{N} = 4$  super Yang-Mills theory. We re-examine two circular Wilson loops and describe how the phase transition occurs in the presence of deformation parameter.

# 1 Introduction

The solution-generating technique [1] provides a new gravity solution which is dual to marginally deformed field theories. The deformed solution preserves  $\mathcal{N} = 1$  supersymmetry as long as the direction corresponding to  $U(1)_R$  R-symmetry is not involved in this procedure.

This method can be also used to find the gravity dual of deformed Coulomb branch RG flow of  $\mathcal{N} = 4$  super Yang-Mills theory where this part of moduli space corresponds to a continuous distribution of D3-branes on an ellipsoidal shell [2]. The UV limit of the dual gauge theory is the Leigh-Strassler deformation [3] of  $\mathcal{N} = 4$  super Yang-Mills theory.

Recently, in [4], for certain moduli space, the  $\sigma$  deformation induces a transition from Coulombic attraction between quark and anti-quark to linear confinement where the scale of confinement increases with this deformation parameter  $\sigma$ . Moreover, this method can also be used to the case of massive quark and monopole [5] and the Wilson loop computation implies that either this deformation enhances the Coulombic attraction or it induces a phase transition to linear confinement.

Gross and Ooguri [6] have found a phase transition where the classical minimal surface can have a topology of annulus or consists of two disconnected surfaces. When the distance between the loops are very small, then the area of annulus is smaller than the one of disconnected surfaces. As the distance increases, the area of annulus also increases. At some critical distance, the disconnected surface becomes more dominant. This jump from one saddle point to the other should lead to a phase transition in the Wilson loop correlator. This configuration was studied in  $AdS_5$  space in [7] by solving the equations of motion where two concentric circles of equal radii were considered. For certain value of distance, the classical connected solution ceases to exist. In other words, the connected minimal surface becomes unstable at this value. The exact critical point where the areas of connected surface and disconnected surface are equal to each other is less than this value. For the unequal radii, similar analysis was done in [8] and the finite temperature case was analyzed in [9].

In this paper, we re-compute two circular Wilson loop case originated from [7] in the marginally deformed  $AdS_5 \times S^5$  type IIB background. After describing equal radii, then we also study the different radii case. Starting with Lunin-Maldacena deformed metric [1], one can construct Nambu-Goto action and its equations of motion. Given the appropriate boundary conditions, the distance between the two loops is a function of an integration constant by elliptic integrals and we present its behavior under the deformation parameter explicitly. Similarly, the area of minimal connected and disconnected surfaces can be constructed and we describe its behavior with respect to the distance between the loops by changing the

deformation parameter.

## 2 Two circular Wilson loops revisited

The Wilson loop correlator can be expressed as an area of the classical string worldsheet stretched between the loops. Let us consider two Wilson loops in the boundary of  $AdS_5$  and they are concentric circles of radius  $R$  (or  $R_1$  and  $R_2$  for unequal radii) separated by a distance  $L$  [6, 7].

The Lunin-Maldacena deformation [1] of  $AdS_5 \times S^5$  background of type IIB theory has the string frame metric

$$ds_{str}^2 = \alpha' \sqrt{H} \left( U^2 dx_\mu^2 + \frac{dU^2}{U^2} + ds_{\tilde{S}^5}^2 \right), \quad H = 1 + \hat{\sigma}^2, \quad \hat{\sigma} \equiv \sigma/2$$

where we set the length scale of  $AdS_5$  to one. The conformal factor  $H \geq 1$  becomes a constant [4] after using the equations of motion for internal coordinates on five-sphere  $\tilde{S}^5$  which depends on the modulus of complex  $\beta$ . This  $\beta$  can be realized by two real deformation parameters  $\gamma$  and  $\sigma$ . The string tension  $1/(2\pi\alpha')$  is proportional to the Yang-Mills coupling  $g_{YM}$ . The Euclidean  $AdS_5$  metric can be written in terms of cylindrical coordinates [7] which are appropriate for the symmetry of Wilson loops above we are considering, by using a change of variable  $z \equiv 1/U$  (the  $AdS_5$  boundary is located at  $z = 0$ ),

$$ds_E^2 = \alpha' \frac{\sqrt{H}}{z^2} (dt^2 + dz^2 + dx^2 + dr^2 + r^2 d\phi^2).$$

The Nambu-Goto action for a fundamental string on the type IIB supergravity background from the ansatz [7] for the minimal surface  $t = 0, \phi = \sigma, r = r(\tau), x = x(\tau)$  and  $z = z(\tau)$  is

$$S = 2\pi \int d\tau \frac{r}{z^2} \sqrt{H} \sqrt{x'^2 + r'^2 + z'^2} \quad (2.1)$$

where  $'$  denotes a derivative with respect to  $\tau$ . Note that the  $\hat{\sigma} = 0$  limit reproduces the undeformed result [7] because  $H = 1$ .

We would like to study the effects of  $\hat{\sigma}$  deformation on the two Wilson loops by following the procedure of [7]. Since the action does not explicitly depend on  $x$ , the equation of motion for  $x$  implies

$$\frac{r}{z^2} \frac{x'}{\sqrt{x'^2 + r'^2 + z'^2}} \sqrt{H} \equiv k \quad (2.2)$$

which is an integration constant. Note the presence of a factor of  $\sqrt{H}$  which will propagate all the remaining computations. For the positive  $k$ ,  $x'$  is also positive and one can choose the

gauge  $\tau = x$ <sup>1</sup>. Then the Euler-Lagrange equations of motion for  $x, r$  and  $z$  with this gauge choice can be summarized as

$$\begin{aligned} r'^2 + z'^2 + 1 - \frac{r^2}{k^2 z^4} H &= 0, \\ r'' - \frac{r}{k^2 z^4} H &= 0, \\ z'' + \frac{2r^2}{k^2 z^5} H &= 0 \end{aligned} \tag{2.3}$$

where the constant of equation of motion (2.2) is used in the second and third equations. Compared with the undeformed theory [7], the dependence on the deformation parameter  $H$  appears in these equations. Whenever we need to know the undeformed results, we simply put  $H$  as one.

## 2.1 The loops have equal radii

We assume that two circular Wilson loops are located at  $x = \pm L/2$  on the  $AdS_5$  boundary located at  $z = 0$ . Then the boundary conditions for the differential equations (2.3) are characterized by [7]

$$r(-L/2) = r(L/2) = R, \quad z(-L/2) = z(L/2) = 0.$$

$R$  and  $L$  are the radii of the circular Wilson loops and the distance between them respectively. The modified boundary condition of  $z$  will be discussed later. As done in [7] explicitly, the solutions for the last two equations of (2.3) satisfying the boundary conditions are given by

$$r = \sqrt{a^2 - x^2} \cos \theta, \quad z = \sqrt{a^2 - x^2} \sin \theta, \quad a^2 \equiv R^2 + \frac{L^2}{4}. \tag{2.4}$$

Here the parametric angle  $\theta$  from the first equation of (2.3) satisfies

$$\theta' = \pm \frac{a}{a^2 - x^2} \sqrt{\frac{H \cos^2 \theta}{k^2 a^2 \sin^4 \theta} - 1} \tag{2.5}$$

where the upper sign is for the negative  $x$  and the lower sign is for the positive  $x$ . From the above boundary conditions, it is easy to see that  $\theta(-L/2) = \theta(L/2) = 0$  and note the presence of a factor  $H$  inside of the square root. Strictly speaking, the modified boundary condition due to the regularization will be present and will be used later.

---

<sup>1</sup>For  $k = 0$ , the minimal surface in  $AdS_5$  bounded by a circle of radius  $R$  is  $r^2 + z^2 = R^2$  [10, 11]. We will see this case from the discussion of (2.16) by taking  $k = 0$  limit.

By using an integral formula [12, 9],

$$\int_0^\theta d\theta \frac{\sin^2 \theta}{\sqrt{\cos^2 \theta - \frac{k^2 a^2 \sin^4 \theta}{H}}} = \frac{\sqrt{H}}{ka} \frac{\beta_+ - 1}{\sqrt{\beta_+ - \beta_-}} \left[ \Pi \left( \chi, \frac{1 - \beta_-}{\beta_+ - \beta_-}, \kappa \right) - F(\chi, \kappa) \right] \quad (2.6)$$

where  $\Pi$  and  $F$  are the elliptic integrals of the third and first kind, respectively and let us introduce various “deformed” parameters [9] in the sense that we are dealing with  $H$ -dependent quantities

$$\begin{aligned} \beta_\pm &= \frac{\frac{2k^2 a^2}{H} + 1 \pm \sqrt{1 + \frac{4k^2 a^2}{H}}}{\frac{2k^2 a^2}{H}}, & \chi &= \sin^{-1} \sqrt{\frac{(\beta_+ - \beta_-)(1 - \cos^2 \theta)}{(1 - \beta_-)(\beta_+ - \cos^2 \theta)}}, \\ \kappa &= \sqrt{\frac{\beta_+(1 - \beta_-)}{\beta_+ - \beta_-}}, \end{aligned} \quad (2.7)$$

the relation (2.5) provides that the expression (2.6) is equal to

$$\frac{\sqrt{H}}{2ka} \ln \frac{(a + \frac{L}{2})(a \pm x)}{(a - \frac{L}{2})(a \mp x)} \quad (2.8)$$

where the upper sign is for the region  $-\frac{L}{2} \leq x \leq 0$  and the lower sign is for the region  $0 \leq x \leq \frac{L}{2}$ . From (2.8), one can check that  $\theta(-L/2) = \theta(L/2) = 0$ . Note that in the computation of an integral (2.6), it is crucial to identify the relative magnitudes of four roots of the denominator and numerator of an integrand (where we made a change of variable  $\cos^2 \theta$  as new one in (2.6)) and lower limit of an integral. In our case, although the presence of the deformation parameter  $H$  appears in (2.7) explicitly, it is easy to see the relative magnitudes of these five quantities. As in undeformed case [7], there exists a relation  $\beta_+ > 1 \geq \cos^2 \theta \geq \beta_- > 0$ .

In particular, at  $x = 0$ , by eliminating the common factor  $\frac{\sqrt{H}}{ka}$ , one arrives at

$$F(ka) = \frac{1}{2} \ln \left( \frac{a + \frac{L}{2}}{a - \frac{L}{2}} \right) = \ln \left( \frac{\sqrt{R^2 + \frac{L^2}{4}} + \frac{L}{2}}{R} \right) \quad (2.9)$$

where we substituted the expression of  $a$  in (2.4), the function  $F(ka)$  is defined by (2.6) without a factor  $\frac{\sqrt{H}}{2ka}$  and this can be reduced to “deformed” function

$$F(ka) = \frac{\beta_+ - 1}{\sqrt{\beta_+ - \beta_-}} \left[ \Pi \left( \frac{1 - \beta_-}{\beta_+ - \beta_-}, \kappa \right) - K(\kappa) \right] \quad (2.10)$$

together with “deformed” parameters (2.7). Here we use the fact that the parameter  $\chi$  in (2.7) becomes  $\frac{\pi}{2}$  when  $\theta$  at  $x = 0$  satisfies  $\cos^2 \theta = \beta_-$  [7]. This enables us to write  $F(ka)$  in terms

of the complete elliptic integrals as above. After differentiating this  $F(ka)$  with respect to  $ka$  and putting it to zero, one gets  $K(\kappa) = 2E(\kappa)$  where the explicit form of  $\kappa^2$  in (2.7) is

$$\kappa^2 = \frac{1}{2} \left( 1 + \frac{1}{\sqrt{1 + 4\frac{k^2 a^2}{1 + \hat{\sigma}^2}}} \right). \quad (2.11)$$

Numerically, this  $\kappa^2$  becomes 0.826 satisfying the condition  $K(\kappa) = 2E(\kappa)$  and this leads to

$$ka = 0.58\sqrt{H} = 0.58\sqrt{1 + \hat{\sigma}^2}. \quad (2.12)$$

The  $\hat{\sigma}$  deformations increase  $ka$  for fixed distance  $L$  between the two circular Wilson loops. See Figure 1 for details. For large  $ka$ , the above  $F(ka)$  has the following asymptotic behavior, by realizing that the third kind of complete elliptic integral can be reduced to the second kind one,

$$F(ka) = \frac{H^{1/4}}{\sqrt{2ka}} \left[ 2E\left(\frac{1}{\sqrt{2}}\right) - K\left(\frac{1}{\sqrt{2}}\right) \right] = \frac{H^{1/4}}{\sqrt{2ka}} \frac{2\pi^{3/2}}{\Gamma^2(\frac{1}{4})} \quad (2.13)$$

which approaches zero as  $ka$  becomes very large. Due to the deformation parameter  $H^{1/4}$ , the undeformed case approaches to zero faster than deformed cases. For small  $ka$ , one can expand the elliptic integrals around  $ka = 0$  and arrives at  $F(ka) = -\frac{ka}{\sqrt{1 + \hat{\sigma}^2}} \ln \frac{ka}{\sqrt{1 + \hat{\sigma}^2}}$ . Therefore, the function  $F(ka)$  becomes zero at  $ka = 0$  and due to a factor  $1/\sqrt{H}$ , the “deformed”  $F(ka)$  approaches zero faster than undeformed  $F(ka)$ . See also Figure 2.

Finally, by simplifying (2.9), one gets “deformed” relation between the distance  $L$  and an integration constant  $k$

$$L = 2R \sinh F(ka) \quad (2.14)$$

with “deformed” function  $F(ka)$  (2.10). Although the functional relation of (2.14) looks similar to the one for undeformed theory [7], note that the dependence on the deformation parameter arises from  $\beta_{\pm}$  and  $\kappa$  in (2.7).

Figure 1 shows the  $ka$  dependence of  $L$  when  $R = 1$ . For each undeformed and “deformed” case, there exists a maximal distance  $L_{max}$  between the two circular Wilson loops. This  $L_{max}$  can be obtained by substituting (2.12) with (2.14) and is given by

$$L_{max} = 1.04R \quad (2.15)$$

where the corresponding integration constant is  $ka = 0.58\sqrt{1 + \hat{\sigma}^2}$  and the two branches from large  $ka$  and from small  $ka$  meet at these points. As we pointed out, at these two

extreme cases of  $ka$  the distance  $L$  approaches to zero. Note that the deformation parameter  $H = 1 + \hat{\sigma}^2$  is cancelled out in (2.14) after plugging (2.12) and the above maximal distance  $L_{max}$  is the same as the one in undeformed theory [7]. This is clear from Figure 1. If  $L > L_{max}$ , then the classical connected solution becomes unstable [6] and the physical solutions are two discontinuous ones [6]. As we observed, when  $ka = 0$ , the distance  $L$  goes to zero. In other words, a single circular Wilson loop case can be seen at  $L = 0$ . This will be discussed after the energy (2.16) is determined later. When  $ka$  is very large, the  $\hat{\sigma}$  deformation increases the value of  $ka$  for fixed  $L$  and furthermore increases  $L$  for fixed  $ka$ .

Since the area of connected surface needs to be regularized [7], the boundary condition for  $z$  can be modified as  $z(\pm L/2) = \epsilon$ . Accordingly, the boundary condition for  $\theta(x)$  is changed to  $\theta(\pm L/2) = \tan^{-1}(\frac{\epsilon}{R})$  from (2.4) [7]. The area of the regularized connected surface can be written as <sup>2</sup>

$$\begin{aligned} S &= 2\pi \int_{-\frac{L}{2}}^{\frac{L}{2}} dx \frac{r}{z^2} \sqrt{H} \sqrt{1 + r'^2 + z'^2} = 4\pi \int_{\frac{\epsilon}{R}}^{\theta(x=0)} d\theta \frac{\sqrt{H} \cot^2 \theta}{\sqrt{\cos^2 \theta - \frac{k^2 a^2 \sin^4 \theta}{H}}} \\ &= 4\pi \sqrt{H} \left(1 + \frac{4k^2 a^2}{H}\right)^{1/4} [(1 - \kappa^2)K(\kappa) - E(\kappa)] + \frac{4\pi \sqrt{H} R}{\epsilon} \end{aligned} \quad (2.16)$$

where “deformed”  $\kappa$  is the same as the one in (2.7) or (2.11). We used the equations of motion (2.2), (2.4), and (2.5) in this computation. Compared with the undeformed case [7], the overall factor  $\sqrt{H}$  appears and this will lead to an overall shift of  $S$ . Moreover, the first two terms of (2.16) have “deformed” parameter and this will change the slope of Figure 2 significantly as the  $\hat{\sigma}$  increases. Therefore, two circular Wilson loops correlator can be obtained from (2.10), (2.14), and (2.16). Some results from gauge theory side in perturbation theory were found in [13, 14].

For large  $ka$  (in other words,  $L$  goes to zero) where  $\kappa$  goes to  $\frac{1}{\sqrt{2}}$  from (2.11), the area can

---

<sup>2</sup>In this computation we use the following integral formula [12]:

$$\begin{aligned} \int_C^U \sqrt{\frac{X-D}{(A-X)(B-X)^3(X-C)}} dX &= \frac{2(C-D)F(\Delta, Q)}{(B-C)\sqrt{(A-C)(B-D)}} - \frac{2\sqrt{(A-C)(B-D)}E(\Delta, Q)}{(A-B)(B-C)} \\ &+ \frac{2(B-D)}{(A-B)(B-C)} \sqrt{\frac{(A-U)(U-C)}{(B-U)(U-D)}} \end{aligned}$$

where  $A > B > U > C > D$ ,  $\Delta = \sin^{-1} \sqrt{\frac{(B-D)(U-C)}{(B-C)(U-D)}}$  and  $Q = \sqrt{\frac{(B-C)(A-D)}{(A-C)(B-D)}}$  where  $F$  and  $E$  are elliptic integrals of first and second kind. Then one can easily see the divergent part of  $S$  which originates from the last term of the right hand side above.

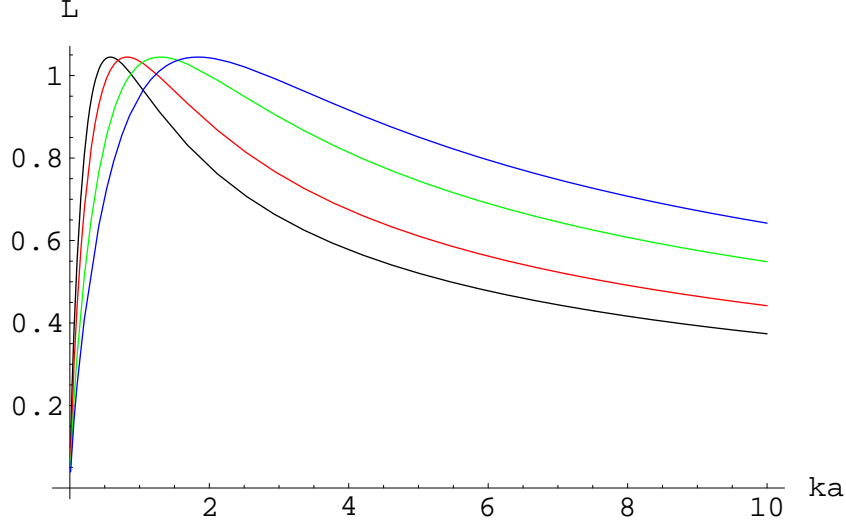


Figure 1: The  $L$  dependence of  $ka$  using (2.14) with (2.10) for  $\hat{\sigma} = 0$ (black), 1(red), 2(green), and 3(blue). These curves for large  $ka$  appear from bottom to top. The maximal distance  $L_{max}$  is given by  $1.04R$  (2.15) where we set  $R = 1$  and the corresponding  $ka$ 's with (2.12) are  $0.58$ ,  $0.82 = 0.58\sqrt{2}$ ,  $1.30 = 0.58\sqrt{5}$ ,  $1.83 = 0.58\sqrt{10}$  respectively. When  $ka$  is large, the  $\hat{\sigma}$  deformation increases the value of  $ka$  for fixed  $L$  and increases  $L$  for fixed  $ka$ . Note that the maximal distance is the same both undeformed( $\hat{\sigma} = 0$ ) case and deformed( $\hat{\sigma} \neq 0$ ) case. The whole curve moves to the right hand side as  $\hat{\sigma}$  increases.

be approximated as

$$S = \frac{4\pi\sqrt{H}R}{\epsilon} - \frac{16\pi^4\sqrt{H}}{\Gamma^4(\frac{1}{4})} \frac{R}{L} = \sqrt{H} \left( \frac{4\pi R}{\epsilon} - \frac{16\pi^4}{\Gamma^4(\frac{1}{4})} \frac{R}{L} \right). \quad (2.17)$$

Here we write  $ka$  in terms of  $L$  through (2.13) and (2.14). This is exactly the minimal surface for anti-parallel lines [15, 16], each of length  $R$  and separated by a distance  $L$  with “deformed” parameter [4]. This indicates that when we consider for the two circular Wilson loop case of ellipsoidal D3-brane distribution with deformation, the similar limiting procedure as above will lead to the minimal surface of deformation of Coulomb branch flow [4]. We will comment on this possibility next section. Therefore, the area of minimal surface is increased by a factor  $\sqrt{H}$  which is greater than or equal to 1.

When  $ka = 0$ ,  $\kappa = 1$  and  $E(1) = 1$ . Then the regular part of (2.16) becomes  $-4\pi\sqrt{H}$  which will be the regular piece of disconnected surface below (2.18).

On the other hand, the area of “deformed” regularized disconnected surface is obtained from the description of [10, 11] by multiplying a factor  $\sqrt{H}$  because the metric has an extra factor  $\sqrt{H}$  which is a constant

$$S_{disc.} = -4\pi\sqrt{H} + \frac{4\pi\sqrt{H}R}{\epsilon}. \quad (2.18)$$

When the regular piece of connected surface and the one for disconnected surface are equal to each other, one can solve the condition for  $ka$  numerically. By equating the first two terms of (2.16) and the first term of (2.18), one gets

$$ka = 1.31\sqrt{H} = 1.31\sqrt{1 + \hat{\sigma}^2} \quad (2.19)$$

for nonzero  $ka$ . By inserting this value into (2.14), one finds the critical distance is given by

$$L_{cri.} = 0.91R$$

which is exactly the same as the one in undeformed case [7] because the deformation parameter is cancelled after substituting (2.19) into (2.14). This critical distance  $L_{cri.}$  is less than the maximal distance  $L_{max}$  (2.15).

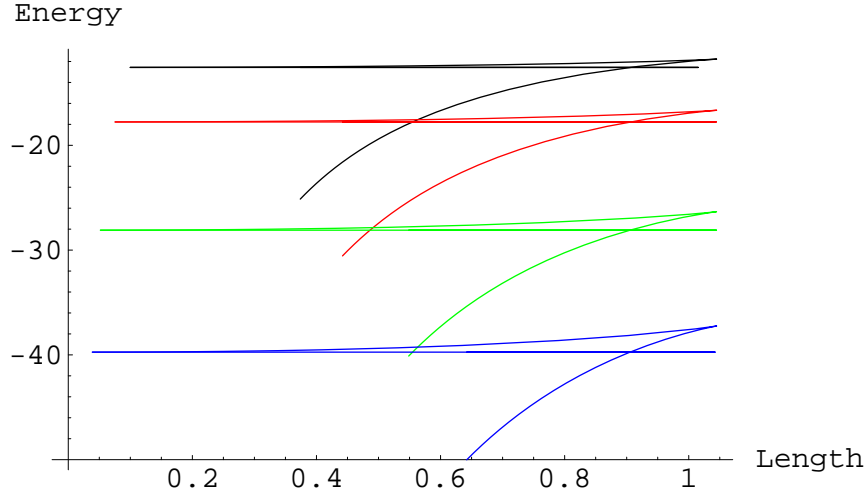


Figure 2: The  $L$  dependence of  $S - \frac{4\pi\sqrt{H}R}{\epsilon}$  characterized by the curves and  $-4\pi\sqrt{H}$  characterized by straight lines using (2.16), (2.18), (2.14) and (2.10) for  $\hat{\sigma} = 0$ (black), 1(red), 2(green), and 3(blue)(from top to bottom). Note the appearance of cusps at the maximal distance  $L_{max} = 1.04R$  where we set  $R = 1$ . The connected surface intersects with disconnected surface at  $L = 0$  and  $L_{cri.} = 0.91R$ . Recall that around  $L = 0$ , as the deformation parameter increases,  $L$  approaches to zero faster(The minimum value of  $L$  for blue one is less than the minimum value  $L$  of black one in the first branch while the opposite holds in the second branch). The  $\hat{\sigma}$  deformation enhances the energy of surface.

Figure 2 describes the  $L$  dependence of the regular parts of  $S$  and  $S_{disc.}$  showing the phase transition at the  $L = L_{cri.}$  Using the parametric plot between these two quantities, we can eliminate the dependence of parameter  $ka$  and obtain the dependence of the regular parts of  $S$  and  $S_{disc.}$  on the distance  $L$  directly. We use the equations (2.16), (2.18), (2.14) and (2.10).

There exist two kinds of branches. The first branch is located in the region between  $L = 0$  and  $L_{max}$  where the cusp appears and the second branch is located in the region between  $L_{max}$  and  $L_{min}$  which is not equal to zero. These two branches for the regular piece of  $S$  intersect with the regular piece of  $S_{disc.}$  at both  $L_{cri.} = 0.91R$  and  $L = 0$ , as we explained above. The location of cusps (the difference between the energy for disconnected minimal surface and the one for connected surface at  $L = L_{max}$ ) are increased as the deformation parameter  $\hat{\sigma}$  increases.

As the deformation parameter  $\hat{\sigma}$  increases, the minimum value  $L_{min}$  of the first branch becomes smaller and the one of second branch becomes larger. This can be understood from the behavior of  $ka$  in the “deformed” function  $F(ka)$ , as we discussed previously: a factor of  $H^{-1/2}$  for small  $ka$  and a factor of  $H^{1/4}$  for large  $ka$ . Before the point  $L_{cri.} = 0.91R$  is reached, the classical connected solution has lower action than the disconnected one and will dominate in the two circular Wilson loop correlator while after that critical point is reached, the disconnected solution will dominate. In other words, the Gross-Ooguri phase transition occurs across this critical point. For fixed length  $L$ , the slopes of the curve (the derivative an energy with respect to th distance) increase as the  $\hat{\sigma}$  increases. This fact reflects the area (2.16) has “deformed” parameter. For the energies, the effect of  $\hat{\sigma}$  enhances the strengths of energies of minimal surface negatively.

## 2.2 The loops have different radii

Two circular Wilson loops are located at  $x = 0$  and  $x = h$  on the  $AdS_5$  boundary. For the unequal radii, the boundary conditions for equations (2.3) are [8]

$$r(0) = R_2, \quad r(h) = R_1, \quad z(0) = z(h) = 0.$$

$R_1$  and  $R_2$  are the radii of the two circular Wilson loops and  $h$  is the distance between them. The solutions with these boundary conditions can be written as [8]

$$\begin{aligned} r &= \sqrt{a^2 - (x + c)^2} \cos \theta, & z &= \sqrt{a^2 - (x + c)^2} \sin \theta, \\ c &\equiv \frac{R_2^2 - R_1^2}{2h} - \frac{h}{2}, & a^2 &\equiv c^2 + R_2^2 \end{aligned}$$

where  $a$  and  $c$  are integration constants. Here there exists a relation

$$\theta' = \pm \frac{a}{a^2 - (x + c)^2} \sqrt{\frac{H \cos^2 \theta}{k^2 a^2 \sin^4 \theta} - 1}$$

where the upper sign is for  $x$  in  $0 < x < x_0$  and lower sign is for  $x$  in  $x_0 < x < h$  for some  $x_0$ . The  $x_0$  and  $h$  can be obtained from the following expressions after  $x$ -integrations: from 0 to

$x_0$  and from  $x_0$  to  $h$  respectively [8]

$$\frac{\sqrt{H}}{2ka} \ln \frac{(a+x_0+c)(a-c)}{(a-x_0-c)(a+c)}, \quad \frac{\sqrt{H}}{2ka} \ln \frac{(a+h+c)(a-x_0-c)}{(a-h-c)(a+x_0+c)}$$

that are equal to  $\theta$ -integration (2.6) respectively. By adding these one gets “deformed” function in terms of  $h$ ,  $R_1$ , and  $R_2$

$$\begin{aligned} F(ka) &= \frac{1}{4} \ln \frac{(a+h+c)(a-c)}{(a-h-c)(a+c)} \\ &= \frac{1}{2} \ln \left( \frac{R_1^2 + R_2^2 + h^2 + \sqrt{(R_2^2 - R_1^2)^2 + h^4 + 2h^2(R_1^2 + R_2^2)}}{2R_1R_2} \right) \end{aligned} \quad (2.20)$$

where  $F(ka)$  is the same as before (2.10).

By simplifying this relation (2.20), the “deformed” distance of two circular Wilson loops for different radii corresponding to (2.14) for equal radii is given by

$$h = R_2 \sqrt{2\alpha [1 + 2 \sinh^2 F(ka)] - \alpha^2 - 1} \quad (2.21)$$

where the ratio of two radii is

$$\alpha \equiv R_1/R_2.$$

As observed in [8], due to the positivity of the inside of the square root, there exists some possible range for the ratio of two radii  $\alpha$ . The maximum value of  $\alpha$  is 2.72 [8]. The maximum value of  $h$  occurs when  $\alpha = 1 + 2 \sinh^2 F(ka)$ . Then  $h_{max}$  can be obtained and it is given by

$$h_{max} = 1.17R_2 \quad (2.22)$$

under the condition (2.12). Of course, when  $\alpha = 1$  (equal radii), the distance  $h$  is reduced to (2.14) with  $R = R_2$ . When both  $h$  and  $ka$  are equal to zero, the solution (2.21) implies that only  $\alpha = 1$  is valid. Other values of  $\alpha$  cannot give simultaneous zero for  $h$  and  $ka$  because there exists an extra term  $(\alpha - 1)^2$  inside of the square root of (2.21) in addition to “deformed” function  $F(ka)$  dependent term. As the deformation parameter  $\hat{\sigma}$  increases, the minimum value  $h$  of the first branch becomes smaller and the one of second branch becomes larger.

One can draw the plot  $ka$  versus  $h$  and it turns out the behavior of the plot for fixed  $\alpha$  looks similar to Figure 1. The main difference is the behavior of near  $ka = 0$ . Of course this region has an unstable branch. Since we are considering  $\alpha = 1.5$  for unequal radii, contrary to the previous case, for small  $ka$ ,  $h$  cannot be zero. We can assume that  $\alpha$  is greater than 1

because for the region of  $\alpha < 1$ , there exists a symmetry under the inversion  $R_1 \leftrightarrow R_2$  and one can use the result from the region of  $\alpha > 1$ . As observed in Figure 3, the arc length from the lowest position near  $ka = 0$  to the highest position where the distance  $h$  has its maximum value  $h_{max}$  is less than the one in equal radii case. This can be seen from the next Figure 4 also. The behavior of  $h$  near  $ka = 0$  and large  $ka$  can be read off from (2.21) by inserting the asymptotic expression for  $F(ka)$  at these two regimes. Evidently,  $h$  cannot be zero due to the presence of  $(\alpha - 1)^2$  inside of the square root as we mentioned before.

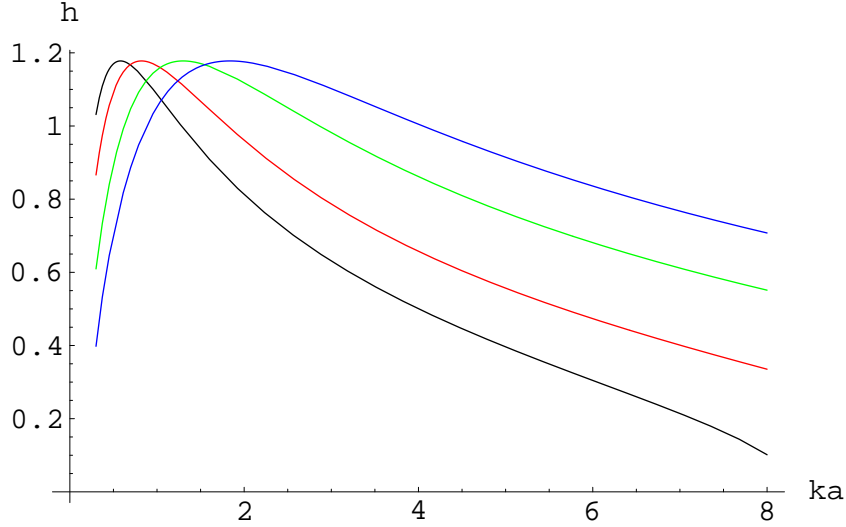


Figure 3: The  $h$  dependence of  $ka$  with  $\alpha = R_1/R_2 = 1.5$  using (2.21) and (2.10) for  $\hat{\sigma} = 0$ (black), 1(red), 2(green), and 3(blue). The maximal distance  $h_{max}$  (2.22) is given by  $1.17R_2$  where we set  $R_2 = 1$  and the corresponding  $ka$ 's with (2.12) are 0.58,  $0.82 = 0.58\sqrt{2}$ ,  $1.30 = 0.58\sqrt{5}$ ,  $1.83 = 0.58\sqrt{10}$  respectively. The  $\hat{\sigma}$  deformation increases the value of  $ka$  for fixed  $h$ . Note that the maximal distance is the same both undeformed( $\hat{\sigma} = 0$ ) case and deformed( $\hat{\sigma} \neq 0$ ) case. For  $\alpha \neq 1$ , the asymptotic behavior for large and small  $ka$  leads to a nonzero  $h$ . The whole curve moves to the right hand side as  $\hat{\sigma}$  increases.

For the area of minimum surface, the boundary conditions for  $\theta$  are characterized by  $\theta(x = 0) = \tan^{-1}(\frac{\epsilon}{R_2})$  and  $\theta(x = h) = \tan^{-1}(\frac{\epsilon}{R_1})$  [8]. The regularized area of the connected surface can be obtained similarly

$$\begin{aligned}
S &= 2\pi \int_0^h dx \frac{r}{z^2} \sqrt{H} \sqrt{1 + r'^2 + z'^2} = 2\pi \left( \int_{\frac{\epsilon}{R_2}}^{\theta(x=x_0)} + \int_{\frac{\epsilon}{R_1}}^{\theta(x=x_0)} \right) d\theta \frac{\sqrt{H} \cot^2 \theta}{\sqrt{\cos^2 \theta - \frac{k^2 a^2 \sin^4 \theta}{H}}} \\
&= 4\pi \sqrt{H} \left( 1 + \frac{4k^2 a^2}{H} \right)^{1/4} [(1 - \kappa^2)K(\kappa) - E(\kappa)] + \frac{2\pi \sqrt{H}(R_1 + R_2)}{\epsilon}
\end{aligned} \tag{2.23}$$

where  $\theta(x = x_0) = \cos^{-2} \beta_-$  with (2.7) and the first two terms are the same expression for equal radii case.

For large  $ka$ , as we did previously, by rewriting  $ka$  in terms of  $\sinh F$  (therefore  $h, R_1$  and  $R_2$  from (2.21) in this case), the area can be written as

$$S = \frac{2\pi\sqrt{H}(R_1 + R_2)}{\epsilon} - \frac{16\pi^4\sqrt{H}}{\Gamma^4(\frac{1}{4})} \sqrt{\frac{R_1 R_2}{(R_1 - R_2)^2 + h^2}}$$

which reduces to (2.17) when  $R_1 = R_2$ . There is also an overall factor  $\sqrt{H}$ . On the other hand, for small  $ka$ , as we observed before, the regular part of (2.23) becomes  $-4\pi\sqrt{H}$  which is the regular piece of disconnected surface (2.18).

By equating the first two terms of (2.23) and the first term of (2.18), one gets  $ka = 1.31\sqrt{1 + \hat{\sigma}^2}$  for nonzero  $ka$  which is the same condition as equal radii case. By inserting this value into (2.21), one finds

$$h_{cri.} = 0.99R_2$$

which is exactly the same as the one in undeformed case [8] and is less than the maximal distance  $h_{max}$  (2.22).

Figure 4 describes the  $h$  dependence of the regular parts of  $S$  and  $S_{disc.}$  showing the phase transition at the  $h = h_{cri.}$ . The regular piece of  $S$  intersects with the regular piece of  $S_{disc.}$  at  $h_{cri.} = 0.99R_2$ , as we explained above. As the deformation parameter  $\hat{\sigma}$  increases, the minimum value of the first branch becomes smaller and the one of second branch becomes larger, like as equal radii case. For the energies, the effect of  $\hat{\sigma}$  enhances the strengths of energies of minimal surface.

### 3 Discussion

First, we have found the “deformed” expression for the distance  $L$  between two circular Wilson loops in terms of the radius  $R$  and an integration constant  $k$  by (2.14), (2.10) and (2.7). Secondly, we also have found the “deformed” energy of minimal surfaces for connected and disconnected ones by (2.16) and (2.18) respectively. They are described by two figures, Figure 1 and Figure 2. We have extended our result to the unequal radii case and they are given by (2.21), (2.10) and (2.23) together with Figure 3 and Figure 4.

For nonconformal theories, the Nambu-Goto action for a fundamental string on the type IIB supergravity background for the minimal surface can be generalized to

$$S = 2\pi \int d\tau \frac{r}{z^2} \sqrt{H L_1 L_2} \sqrt{x'^2 + r'^2 + \frac{1}{L_1 L_2^2} z'^2}, \quad L_i = 1 + \ell_i^2 z^2,$$

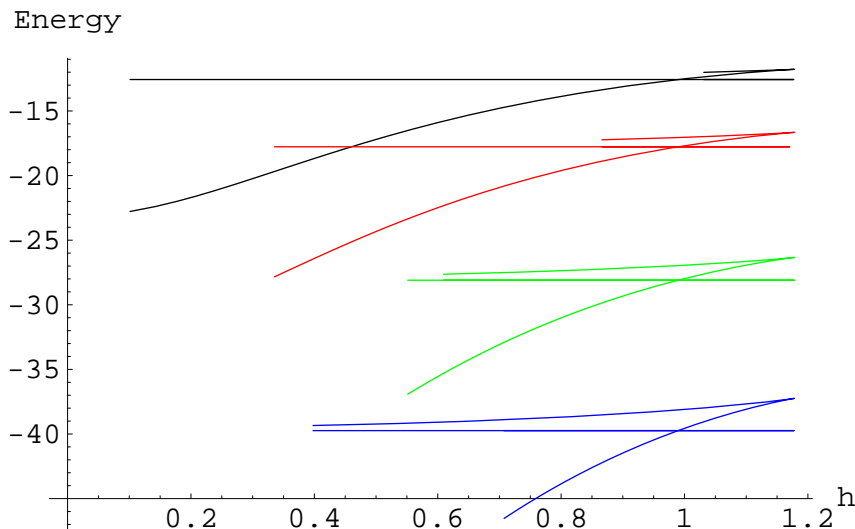


Figure 4: The  $h$  dependence of  $S - \frac{2\pi\sqrt{H}(R_1+R_2)}{\epsilon}$  characterized by the curves and  $-4\pi\sqrt{H}$  characterized by straight lines using (2.23) and (2.18) for  $\hat{\sigma} = 0$ (black), 1(red), 2(green), and 3(blue). We take  $\alpha = R_1/R_2 = 1.5$ . Note the appearance of cusps at the maximal distance  $h_{max} = 1.17R_2$  where we set  $R_2 = 1$ . The connected surface intersects with disconnected surface at  $h_{cri.} = 0.99R_2$ . Recall that around  $h = 0$ , as the deformation parameter increases,  $h$  approaches to zero faster. The  $\hat{\sigma}$  deformation enhances the area of surface.

where  $\ell_i$  are two parameters specifying the ellipsoidal shape of D3-brane distribution [17]. Of course, the vanishing  $\ell_i$  case reduces to (2.1) for the conformal theory we have discussed so far. Then one can construct the Euler-Lagrange equations of motion which is a generalization of (2.3). Although the analytic solutions are not possible, one expects that the similar analysis to [9] can be done numerically and by tuning the parameters and deformation parameter appropriately, one might see the transition to a linearly confining phase.

In [18], through a stereographic projection by conformal transformation, two concentric circles on parallel planes we are considering in this paper define a 2-sphere in  $\mathbf{R}^4$  with different values for the 5-sphere angle. It would be interesting to study our analysis here for the nonzero difference of 5-sphere angles. Moreover, the generalization of [19] in the case of a line or circle with periodic motion inside an  $\mathbf{S}^2$  is given in [18] and some periodic motion inside an  $AdS_3 \times \mathbf{S}^3$  subspace is also given. Some of the simple solution was given already in [20]. It is natural to ask how the marginal deformation plays the role in these examples.

One can consider the  $\hat{\sigma}$  deformations of finite temperature theories which are described by nonextremal D3-branes. For undeformed case with finite temperature case, the analysis was given already in [9]. The  $L_{max}$  and  $L_{cri.}$  with nonzero temperature are increased as the temperature increases and the plot of an energy versus the distance implies that the effect of

temperature leads to an enhancement of an area of minimal surface.

As pointed out in [21], it is straightforward to apply the present description to other types of Sasaki-Einstein spaces for the 5-dimensional internal space. For example, for the  $T^{1,1}$  space, the deformation parameter has similar functional form [21] except that the numerical coefficient of  $\hat{\sigma}^2$  in  $H$  has different value. So we do expect to have similar results.

### Acknowledgments

We would like to thank Nadav Drukker, DaeKil Park, Justin F. Vazquez-Poritz and Konstantin Zarembo for discussions. This work was supported by grant No. R01-2006-000-10965-0 from the Basic Research Program of the Korea Science & Engineering Foundation.

### References

- [1] O. Lunin and J. Maldacena, “Deforming field theories with  $U(1) \times U(1)$  global symmetry and their gravity duals,” JHEP **0505**, 033 (2005) [arXiv:hep-th/0502086].
- [2] C. Ahn and J. F. Vazquez-Poritz, “Deformations of flows from type IIB supergravity,” Class. Quant. Grav. **23**, 3619 (2006) [arXiv:hep-th/0508075].
- [3] R. G. Leigh and M. J. Strassler, “Exactly marginal operators and duality in four-dimensional  $N=1$  supersymmetric gauge theory,” Nucl. Phys. B **447**, 95 (1995) [arXiv:hep-th/9503121].
- [4] C. Ahn and J. F. Vazquez-Poritz, “From marginal deformations to confinement,” [arXiv:hep-th/0603142].
- [5] C. Ahn, “Quark-monopole potentials from supersymmetric  $SL(3, \mathbb{R})$  deformed IIB supergravity,” [arXiv:hep-th/0605012].
- [6] D. J. Gross and H. Ooguri, “Aspects of large  $N$  gauge theory dynamics as seen by string theory,” Phys. Rev. D **58**, 106002 (1998) [arXiv:hep-th/9805129].
- [7] K. Zarembo, “Wilson loop correlator in the AdS/CFT correspondence,” Phys. Lett. B **459**, 527 (1999) [arXiv:hep-th/9904149].
- [8] P. Olesen and K. Zarembo, “Phase transition in Wilson loop correlator from AdS/CFT correspondence,” [arXiv:hep-th/0009210].

- [9] H. Kim, D. K. Park, S. Tamarian and H. J. W. Muller-Kirsten, “Gross-Ooguri phase transition at zero and finite temperature: Two circular Wilson loop case,” JHEP **0103**, 003 (2001) [arXiv:hep-th/0101235].
- [10] N. Drukker, D. J. Gross and H. Ooguri, announced by Gross at the conference, Strings ‘98, <http://www.itp.ucsb.edu/online/strings98/gross/oh/10.html>.
- [11] D. Berenstein, R. Corrado, W. Fischler and J. M. Maldacena, “The operator product expansion for Wilson loops and surfaces in the large N limit,” Phys. Rev. D **59**, 105023 (1999) [arXiv:hep-th/9809188].
- [12] I. S. Gradshteyn and I. M. Ryzhik, Table of integrals, series and products, Sixth Edition, Academic Press, New York, 2000.
- [13] J. Plefka and M. Staudacher, “Two loops to two loops in  $N = 4$  supersymmetric Yang-Mills theory,” JHEP **0109**, 031 (2001) [arXiv:hep-th/0108182].
- [14] G. Arutyunov, J. Plefka and M. Staudacher, “Limiting geometries of two circular Maldacena-Wilson loop operators,” JHEP **0112**, 014 (2001) [arXiv:hep-th/0111290].
- [15] J. M. Maldacena, “Wilson loops in large N field theories,” Phys. Rev. Lett. **80**, 4859 (1998) [arXiv:hep-th/9803002].
- [16] S. J. Rey and J. T. Yee, “Macroscopic strings as heavy quarks in large N gauge theory and anti-de Sitter supergravity,” Eur. Phys. J. C **22**, 379 (2001) [arXiv:hep-th/9803001].
- [17] P. Kraus, F. Larsen and S. P. Trivedi, “The Coulomb branch of gauge theory from rotating branes,” JHEP **9903**, 003 (1999) [arXiv:hep-th/9811120].
- [18] N. Drukker and B. Fiol, “On the integrability of Wilson loops in  $AdS(5) \times S^5$ : Some periodic ansatze,” JHEP **0601**, 056 (2006) [arXiv:hep-th/0506058].
- [19] K. Zarembo, “Supersymmetric Wilson loops,” Nucl. Phys. B **643**, 157 (2002) [arXiv:hep-th/0205160].
- [20] A. A. Tseytlin and K. Zarembo, “Wilson loops in  $N = 4$  SYM theory: Rotation in  $S(5)$ ,” Phys. Rev. D **66**, 125010 (2002) [arXiv:hep-th/0207241].
- [21] J. F. Vazquez-Poritz, “Enhancing the Jet Quenching Parameter from Marginal Deformations,” [arXiv:hep-th/0605296].